AIAA Guidance, Navigation, and Control Conference
08 - 11 August 2011, Portland, Oregon

AIAA 2011-6726

Solar Dynamics Observatory Guidance, Navigation, and Control System Overview

Wendy M. Morgenstern*, Kristin L. Bourkland†, Oscar C. Hsu‡, Dr. Kuo-Chia Liu§, Dr. Paul A. C. Mason**, Dr. James R. O'Donnell Jr.††, Angela M. Russo‡‡, Scott R. Starin§§, and Melissa F. Vess***
NASA Goddard Space Flight Center, Greenbelt, MD 20771, USA

The Solar Dynamics Observatory (SDO) was designed and built at the Goddard Space Flight Center, launched from Cape Canaveral on February 11, 2010, and reached its final geosynchronous science orbit on March 16, 2010. The purpose of SDO is to observe the Sun and continuously relay data to a dedicated ground station. The driving requirements for the Guidance, Navigation and Control (GN&C) system were to achieve geosynchronous orbit; to maintain near-constant Sun observations with 2 arcsec, 3σ, control accuracy; to combine the onboard attitude determination system with a high accuracy solar ephermeris to meet the Attitude Control System's (ACS's) attitude knowledge requirements of [35,70,70] arcsec, 3σ, relative to the center of the solar disk; and to provide an extremely low jitter observation platform despite significant disturbances from the instrument mechanisms, the control actuators and the continual HGA motion required to maintain constant contact with the dedicated ground station.

Along with these challenging requirements came several driving constraints. Mission success required 99% of the science data be successfully downlinked, leaving little time for propulsive maneuver interruptions necessary to maintain the low wheel actuator speeds required to minimize jitter. When a mechanical isolation system proved prohibitive to add to the design, the Flight Dynamics team developed a wheel speed prediction product which allowed the team to 'double' the time between momentum unload maneuvers by precisely targeting the post-unload momentum state so the anticipated environmental torques initially drive the system momentum magnitude towards zero. To take advantage of this, the ACS team tightened the Delta-H controller's accuracy requirements. When grounds tests showed the HGA stepper motors were the dominant jitter source and neither motor operation nor mechanical isolation were viable options, the ACS team added a number of jitter mitigation features to the HGA pointing controller. Finally, when systems testing showed the Inertial Reference Unit's (IRU's) analog internal temperature controller created a dangerous interference with the power subsystem's battery charge controller, the ACS team found a way to meet the challenging attitude stability and knowledge requirements without the rate sensor's drift stabilizing internal temperature control.

This paper details the final overall design of the SDO GN&C system and how it was used in practice during SDO launch, commissioning, and nominal operations. This overview includes the ACS control modes, attitude determination and sensor calibration, the high gain antenna (HGA) calibration and jitter mitigation operation and touches on significant anomalies such as unexpected propellant slosh dynamics and attitude determination issues.

Downloaded by Scott Starin on September 21, 2012 | http://arc.aiaa.org | DOI: 10.2514/6.2011-6726

* GNC Systems Engineer, Attitude Control Systems Engineering Branch/Code 591, AIAA Member
† ACS Analyst, Attitude Control Systems Engineering Branch/Code 591
‡ ACS Analyst, Attitude Control Systems Engineering Branch/Code 591, AIAA Member
§ ACS Analyst, Attitude Control Systems Engineering Branch/Code 591, AIAA Lifetime Member
** ACS Analyst, Attitude Control Systems Engineering Branch/Code 591, AIAA Member
†† Branch Chief, Attitude Control Systems Engineering Branch/Code 591, AIAA Member
‡‡ Systems Engineer, Mission Systems Engineering Branch/Code 599
§§ Associate Branch Head, Attitude Control Systems Engineering Branch/Code 591, AIAA Member
*** ACS Analyst, Attitude Control Systems Engineering Branch/Code 591, AIAA Member

This material is declared a work of the U.S. Government and is not subject to copyright protection in the United States.

I. Introduction

The Solar Dynamics Observatory (SDO) was successfully launched and deployed from its Atlas V launch vehicle on February 11, 2010. Three months later, on May 16, 2010, the fully commissioned heliophysics laboratory was handed over to Space Systems Mission Operations to begin its science mission. SDO is an Explorer-class mission now operating in a geosynchronous orbit, sending data twenty four hours a day to a dedicated ground station in White Sands, New Mexico. It carries a suite of instruments designed to observe the Sun in multiple wavelengths at unprecedented resolution. The Atmospheric Imaging Assembly (AIA) includes four telescopes with 4096×4096 focal plane CCDs that can image the full solar disk in seven extreme ultraviolet and three ultraviolet-visible wavelengths. The Extreme Ultraviolet Variability Experiment (EVE) collects time-correlated data on the activity of the Sun's corona. The Helioseismic and Magnetic Imager (HMI) enables study of pressure waves moving through the body of the Sun.

II. Overview of the Solar Dynamics Observatory Mission

Figure 1 shows an image of the SDO spacecraft. The side of the spacecraft shown at the top of the figure is its Sun-pointing side. The overall length of SDO along the Sun-pointing axis is 4.5 m and each side of the spacecraft bus is 2.2 m. The span of the deployed solar arrays is 6.25 m. SDO launched with a total mass of 3000 kg, 1400 kg of which was propellant mass.

The science goal of SDO is to provide data to help understand the Sun's magnetic changes, to determine how its magnetic field is generated and structured and how that energy is released. SDO data and analysis will help develop the ability to predict the solar variations and their impact on the Earth. SDO's three instruments measure the properties of the Sun and solar activity. The large number of images and other measurements taken continuously over long periods of time will allow scientists to see the oscillations of the Sun. These patterns can be used to look into and through the Sun. More information about the SDO spacecraft and science mission can be found on the NASA SDO website.[†††]

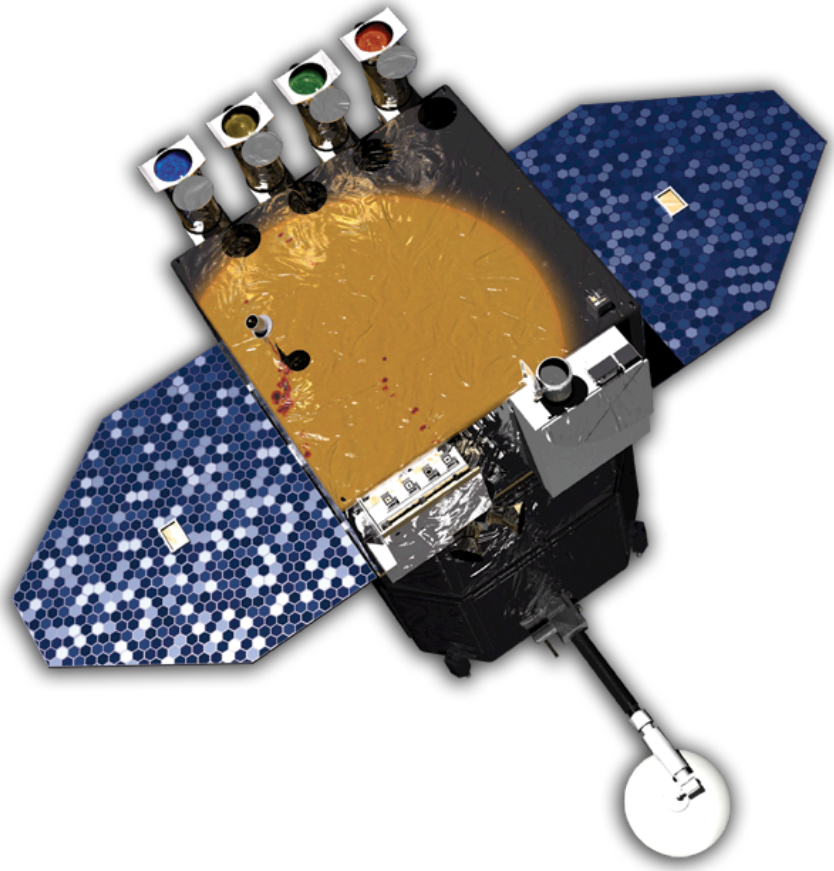

Figure 1: SDO from a sun-facing view

[†††] http://sdo.gsfc.nasa.gov

Downloaded by Scott Starin on September 21, 2012 | http://arc.aiaa.org | DOI: 10.2514/6.2011-6726

Downloaded by Scott Starin on September 21, 2012 | http://arc.aiaa.org | DOI: 10.2514/6.2011-6726

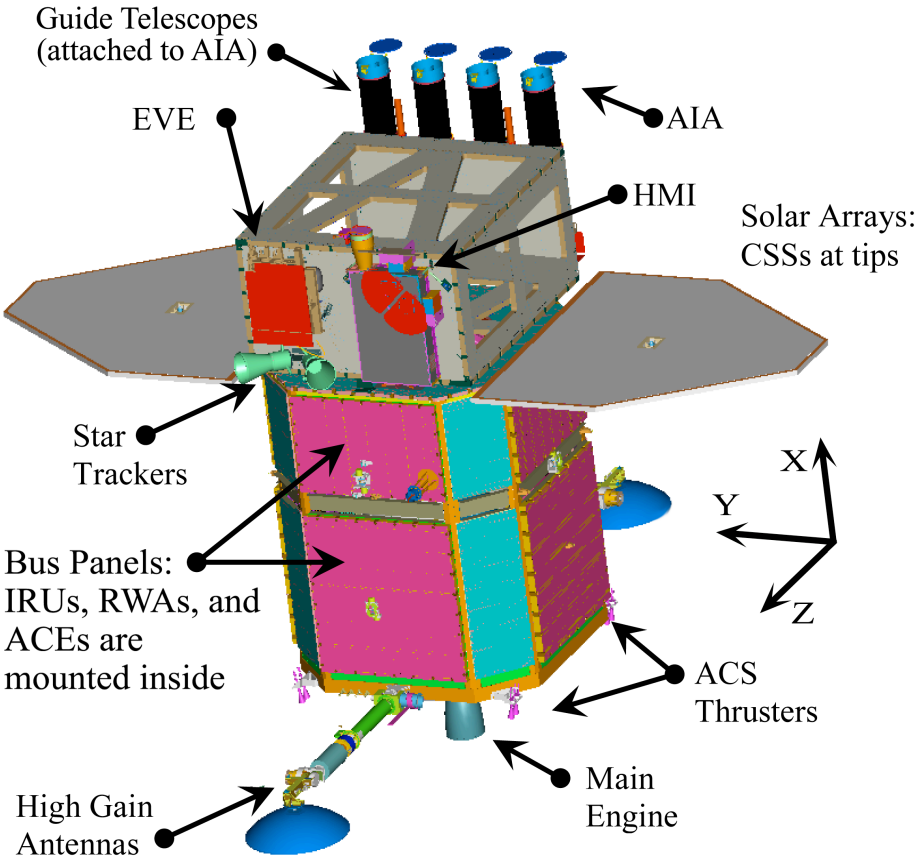

Figure 2: Attitude Control Subsystem Hardware

A. Attitude Control System Sensor and Actuator Suite

Figure 2 shows a mechanical drawing of the spacecraft giving the locations of the attitude control system (ACS) components and science instruments. The SDO ACS was designed to tolerate any single hardware fault and retain the capability to meet all science data quality requirements. The suite of ACS sensors, actuators, and computational capabilities was selected and arranged for performance and maximal redundancy as SDO ACS failure detection and correction (FDC) depends to a large extent on hardware redundancy. More information on the SDO hardware placement can be found in Ref. 1 and an extensive description of the SDO ACS failure detection and correction design can be found in Ref. 2.

The SDO sensor suite consists of sixteen Adcole coarse sun sensors (CSS), one Adcole digital sun sensor (DSS), two Galileo Avionica (GA) autonomous, quaternion-output star trackers (ST), and three Kearfott Two-Axis Rate Assemblies used as SDO's inertial reference units (IRUs). The CSSs are the only attitude sensors required in the most basic Sun-pointing modes. The sixteen CSSs are divided into two independent sets of eight sensors each (CSSA and CSSB), and each set of eight can provide a Sun vector with any seven sensors being functional.

For fine attitude determination an on-board Kalman filter provides adequate attitude knowledge with input from any two of the three fine-pointing units—DSS, ST1, and ST2. To avoid simultaneous blockages of both STs, they are mounted nearly perpendicular to the SDO Sun-pointing axis (X axis), and far enough apart from each other that the Earth and Moon do not block both at the same time throughout the science collection phase of the mission. The IRUs are arranged so that the sensitive axes from any two units are aligned with each of the three body axes of the Observatory. Thus, any two out of three IRUs will provide full three-axis rate information.

In addition to these sensors, the ACS also makes extensive use of the guide telescopes (GT) mounted as part of the AIA instrument. Because of the high accuracy of the SDO science instruments, the ACS uses the GT data as the best available knowledge of the Sun center. There are four GTs, with one mounted to each of the four science telescopes, The ACS only needs accurate information from one of the four GTs, selected by SDO scientists as the controlling guide telescope (CGT), to perform its science control duties. Each GT has a field of view (FOV) of 0.5 deg acquisition range within which the polarity of the control signal is determined when the sunlight illuminates one of the four photodiodes evenly spaced around the circular FOV. When the Sun center is within approximately 90 arcseconds of the FOV center, the GT is capable of providing attitude information relative to the Sun vector accurate to about 2 arcseconds; this is referred to as the GT linear range and is required for accurate science data collection.

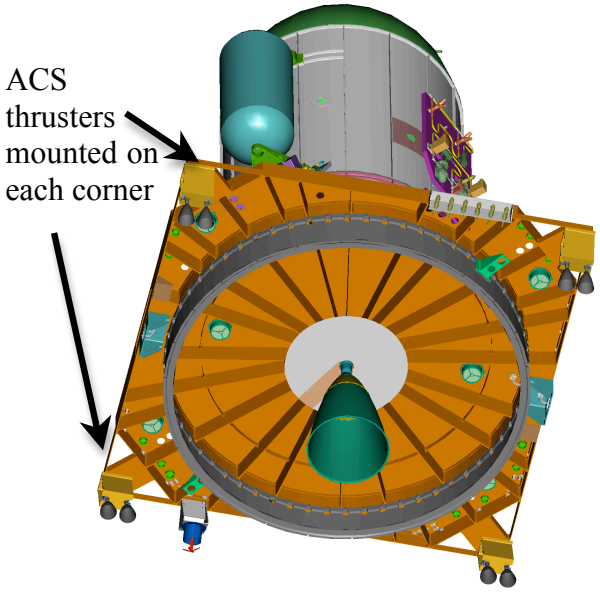

Figure 3: SDO Propulsion Mode, viewed from lower deck

SDO guidance functions are actuated by four Goodrich 70-Nms reaction wheel assemblies (RWA) and eight Ampac 5-lbf attitude control thrusters. While not used for attitude control, there is also one Aerojet R-4D model main engine producing 110 lbf of thrust used for orbit raising ΔV. The RWAs are arranged in a pyramidal structure so that any set of three provides full three-axis control capability. Two 42" circular tanks (PSI 80352) are stacked vertically along the vehicle centerline, containing the fuel (monomethyl hydrazine) and oxidizer (nitrogen tetroxide) bipropellants. The ACS thrusters are physically mounted in four pairs of thrusters on the four corners of the spacecraft lower deck (-X face, anti-Sun direction). One thruster from each pair is assigned to the primary propellant manifold, and the other to the redundant manifold. In this way, the catastrophic failure of any one thruster only requires the closing of one manifold, leaving the other set of four capable of performing all necessary ACS tasks.

In addition to attitude control activities, the ACS is also responsible for the pointing and control of the two high-gain antennas (HGA). Each antenna consists of a dish mounted on dual-axis (elevation and azimuth) gimbals driven by Starsys stepper motors. If either HGA fails due to a gimbal or electrical failure, the

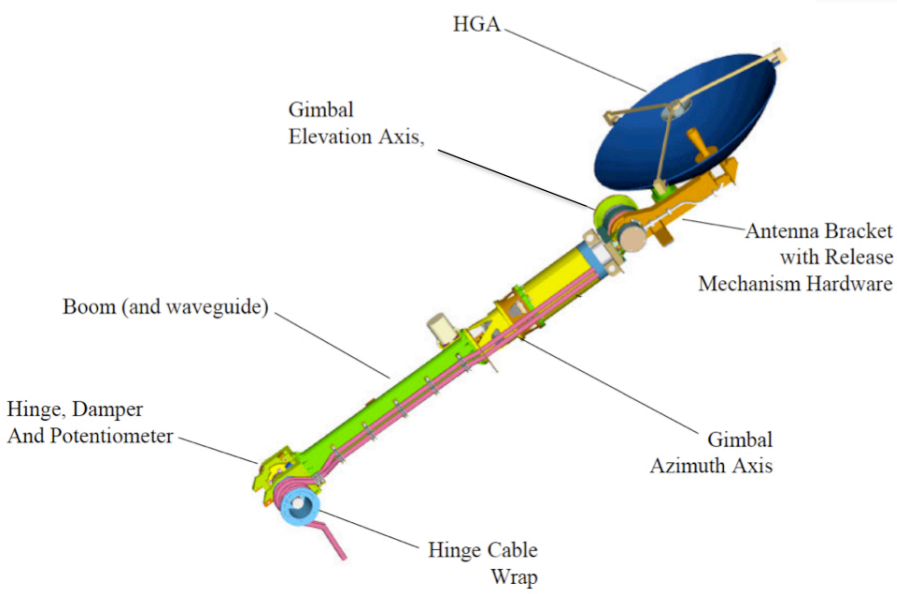

Figure 4: SDO High Gain Antenna assembly

Downloaded by Scott Starin on September 21, 2012 | http://arc.aiaa.org | DOI: 10.2514/6.2011-6726

mission can still be completed. The greatest danger posed by the HGAs is the irradiation of the spacecraft itself and HGA Failure Detection and Correction (FDC) logic provides protection from that event.

B. Electronics and Microprocessors.

A full copy of the command and data handling software of the SDO spacecraft resides on each of two independent main processors (MP) located in the Command & Data Handling (CDH) units (Figure 5). Only one of these MPs is in control of the spacecraft at any time. Each of these MPs also operates an independent copy of the attitude control task (ACT) and the on-board ephemeris. Most flight software tasks, including the ACT, operate on a 200-ms cycle, except that the ephemeris operates on a one-second cycle. Nominally, it is the job of the ACT to sample sensor data and issue actuator commands to maintain attitude control of the spacecraft throughout the mission. There are also separate microprocessors that reside in each of two independent but cross-strapped attitude control electronics (ACE) boxes. These ACEs are always powered, but only one can be in control at any time. Both ACEs route data from the CSSs, RWAs, IRUs, and various pressure and temperature sensors to the MPs. Only the ACE in control accepts, validates, and passes through actuator commands to the RWAs and the propulsion system's valves and thrusters from the MP in control. If there is a disruption of ACT control over the ACE in control, that ACE will cease passing through ACT actuator commands and will instead begin issuing commands to the reaction wheels from the ACE's Safehold controller. Safehold is a simplified mode, being dependent only on the CSSs and the RWA tachometer readings except during eclipse, when the IRU signals, if available, are used to null rates. If the primary ACE itself is disrupted, such as from a restart due to a single-event upset (SEU), the other ACE will detect this state and assume control.

The Gimbal Control Electronics (GCE) functions as the interface to the HGA pointing system. Similar to the ACEs, commands from the MP's HGA pointing control are accepted by the default GCE, validated and passed through to the gimbal motors; antenna position information from the encoders along with hardware status

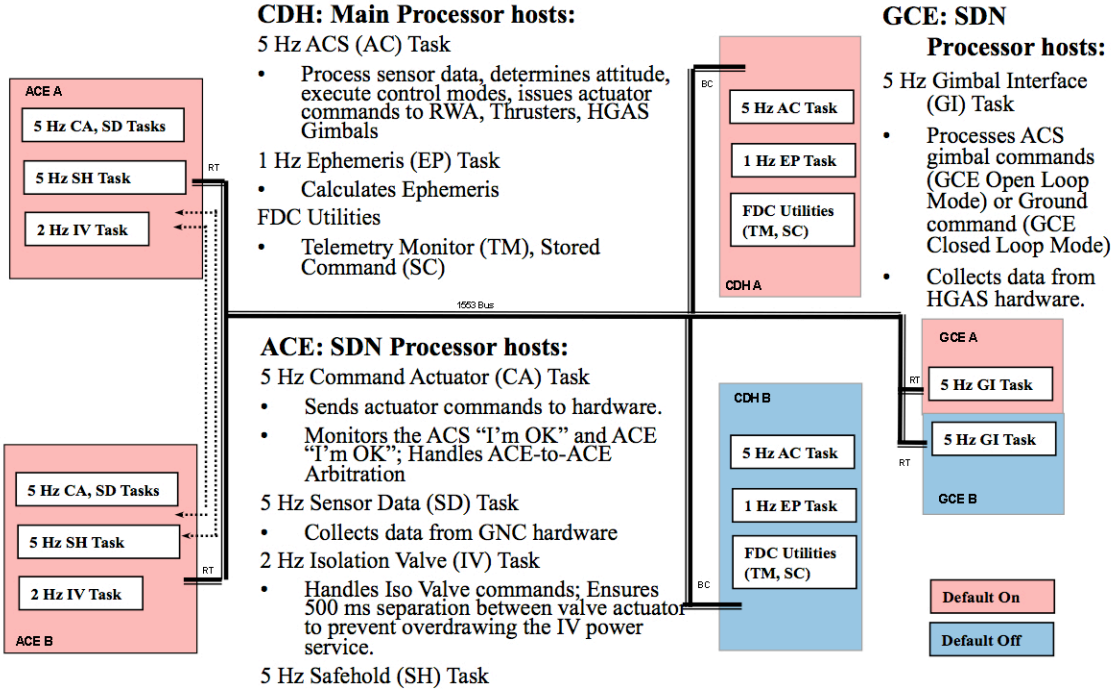

Figure 5: GNC software is distributed across multiple processors

information is returned to the main processor. Unlike the ACE, only one GCE is powered on at a time, so there is no danger of contention for control of the HGA hardware, making safing the HGA subsystem a simple matter of placing the antennas in a safe attitude if there any disruption of ACT control.

Downloaded by Scott Starin on September 21, 2012 | http://arc.aiaa.org | DOI: 10.2514/6.2011-6726

Downloaded by Scott Starin on September 21, 2012 | http://arc.aiaa.org | DOI: 10.2514/6.2011-6726

C. Attitude Control System Mode Design

Figure 6 shows a diagram of the SDO ACS control modes and allowed transitions. The ACS has four RWA-actuated modes and two thruster-actuated modes. More details about the ACS in general and the control modes in particular can be found in Ref.s 1, 3, 4 and 5. As discussed in the previous section, one RWA-actuated mode (Safehold) resides on the ACE microprocessors. The other five modes reside in the ACT. Sun Acquisition (SunAcq) Mode performs an attitude function similar to Safehold, in that it simply maintains a power-positive, safe attitude with respect to the Sun using CSS signals. It differs from Safehold in that IRU signals are used for angular rate information at all times.

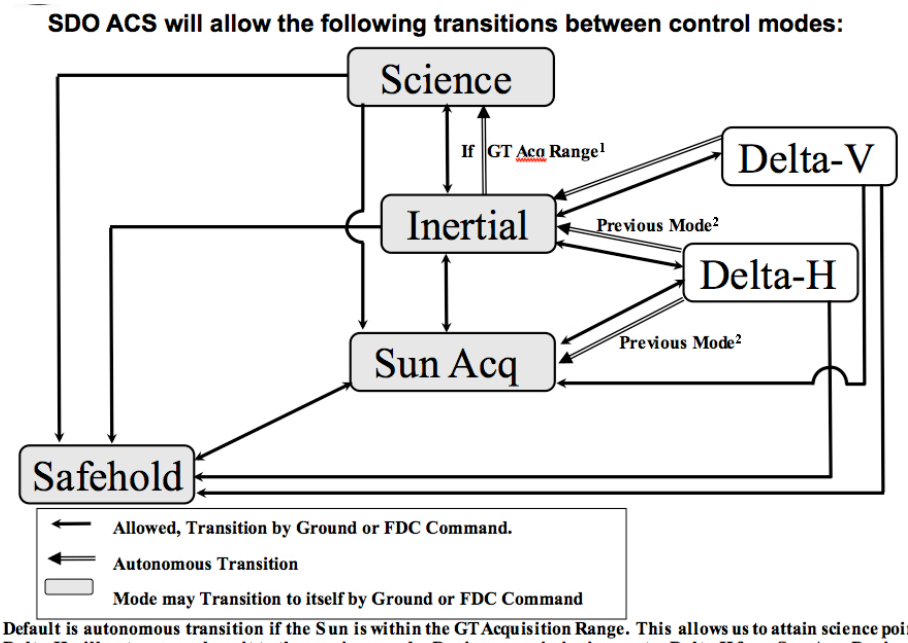

[1] Default is autonomous transition if the Sun is within the GT Acquisition Range. This allows us to attain science pointing quickly.
[2] Delta-H will autonomously exit to the previous mode. During commissioning, enter Delta-H from Sun Acq. During nominal GEO operations, will command from Inertial.

Figure 6: ACS Control Mode Transition Diagram

For all other modes, attitude determination (AD) is performed with some combination of the fine attitude sensors and propagation of IRU-derived rate information. An attitude solution may be initialized either by accepting a valid ST quaternion (nominal) or by uploading an estimate by ground command (available for testing and contingency). Once a solution is available, it may simply be propagated using rate sensors or it may be replaced either using one preferred ST or by ground override command. The most accurate solution is obtained by combining all available fine attitude data from the two STs, the DSS, and the IRUs using a Kalman filter.

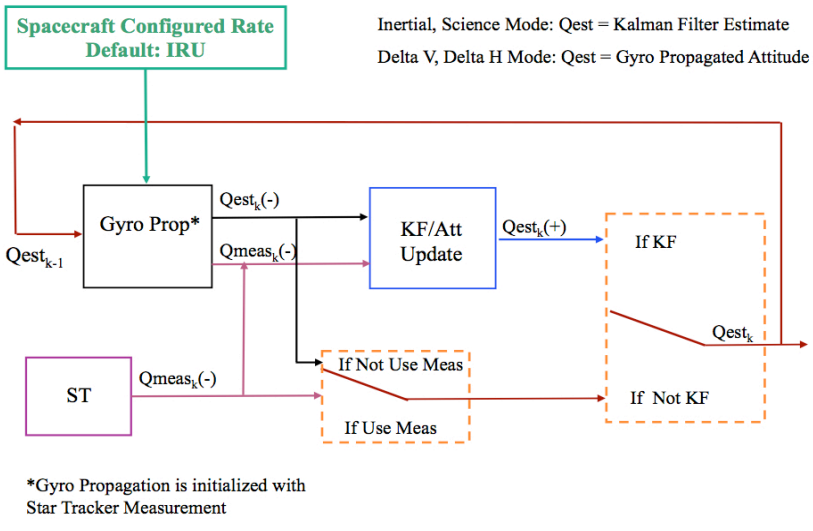

Figure 7: Attitude Determination Diagram

Whatever AD method is selected in the software, Inertial Mode uses the solution for attitude error calculation against the target attitude in all three axes. Inertial has two sub-modes that differ only in the target calculation. One tracks a Sun-referenced target quaternion using the on-board ephemeris to predict the appropriate inertially referenced quaternion for the Sun-referenced state. The other maintains a commanded, absolute, inertially referenced quaternion. Science Mode,

during which most science data are collected, uses one of the specialized GTs to point a commanded science reference boresight (SRB) accurately at the Sun. The roll error about that SRB is calculated using the same methods as Inertial, except that the target is always Sun-referenced.

The thruster modes are called DeltaH Mode and DeltaV Mode. DeltaH is used to manage system angular momentum. With no magnetic torquers to gradually dump momentum, the thrusters must be used occasionally to remove momentum. The attitude target for DeltaH is simply the attitude estimate at mode entry, causing the observatory to hold the current attitude during unloading. To maximize time between uses of DeltaH, the mode allows a non-zero angular momentum to be placed into the body. In order to meet both the jitter requirements and the data completeness budget, it was necessary to take advantage of this design flexibility by setting the momentum target to the opposite of the predicted angular momentum change. This will be discussed further in later sections. DeltaV is used for changing or maintaining orbit parameters. It uses an absolute, inertially referenced target similar to Inertial's absolute targeting, and that target may be updated by command during a DeltaV maneuver.

Some transitions between modes are not allowed. By placing the in-control ACE into Safehold mode, the ACS mode running on the MP is ignored, so Safehold may be reached from any MP mode. Any MP mode may transition to SunAcq or to Inertial, including self-transitions. Science mode may self-transition, and it may also be entered autonomously from Inertial mode when the Sun is in the field-of-view of the controlling guide telescope. DeltaH may be entered from SunAcq or Inertial mode. However, Science and DeltaV may only be entered from Inertial mode, with Science accessible only when Sun-referenced targeting is active and DeltaV accessible only when absolute targeting is active. These restrictions avoid large attitude changes occurring due only to misunderstandings of the two targeting sub-modes in Inertial. Thrusters are always disabled upon exiting DeltaH or DeltaV modes.

Downloaded by Scott Starin on September 21, 2012 | http://arc.aiaa.org | DOI: 10.2514/6.2011-6726

III. Launch and Initial Acquisition

After a one day launch slip caused by high winds at Cape Canaveral, SDO successfully launched at 15:23 GMT (10:23 EST) on February 11, 2010. On schedule an hour and thirty-six minutes later, the SDO Mission Operations Center established first contact with the spacecraft. At 17:07:39, SDO separated from the third stage of the Atlas V launch vehicle, having been safely delivered into its 8,800 km × 41,700 km, 28° geostationary transfer orbit. Figure 8 shows the SDO spacecraft rates leading up to and after spacecraft separation. (All times in plots are GMT.) The angular rates measured prior to separation are due to the third stage of the launch vehicle maneuvering SDO into its separation attitude. As shown, the separation event itself is relatively benign, imparting fairly low rates on the spacecraft, a total of 3 Nms of system momentum. SDO's solar arrays deployed automatically approximately five seconds after separation. Figure 9 shows the Sun angle, as measured by the CSSs, during initial acquisition. The requirement at initial acquisition for both SDO's SunAcq and Safehold Modes was to bring the spacecraft within 15° of the Sun within 30 minutes. In operation, SDO's SunAcq Mode was able to bring the spacecraft that close to the Sun within 15 seconds, with a total settling time of about three minutes. Note that, since the CSSs are located on the solar array panels, the Sun angles were not accurate until the solar arrays were deployed.

Eighty-four minutes after separation, SDO's two HGAs were deployed. Figure 10 shows the spacecraft rate disturbance caused as each antenna was deployed. As expected, the primary disturbance is in the Y axis of the spacecraft.

Downloaded by Scott Starin on September 21, 2012 | http://arc.aiaa.org | DOI: 10.2514/6.2011-6726

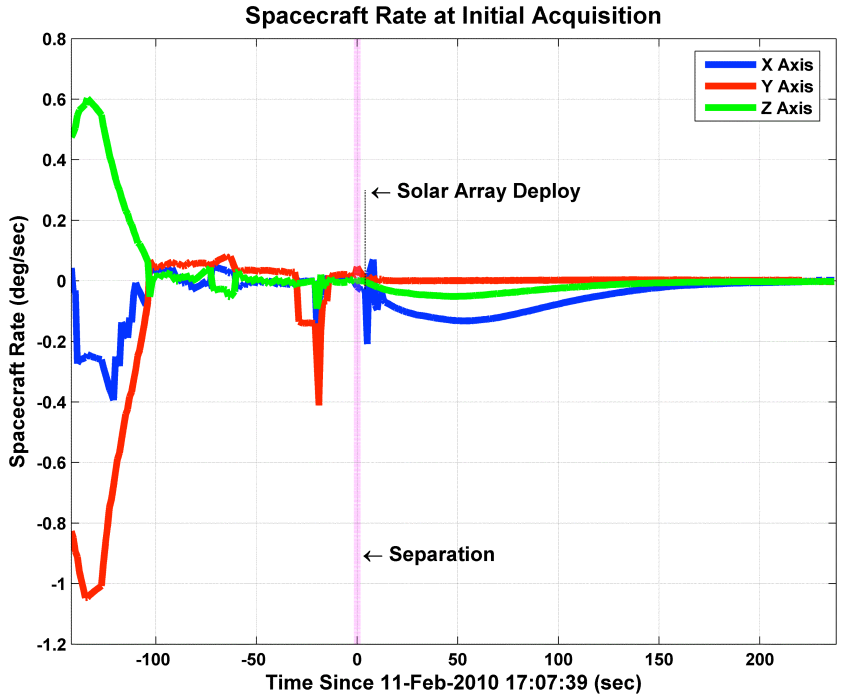

Figure 8: Separation and Acquisition Spacecraft Rates

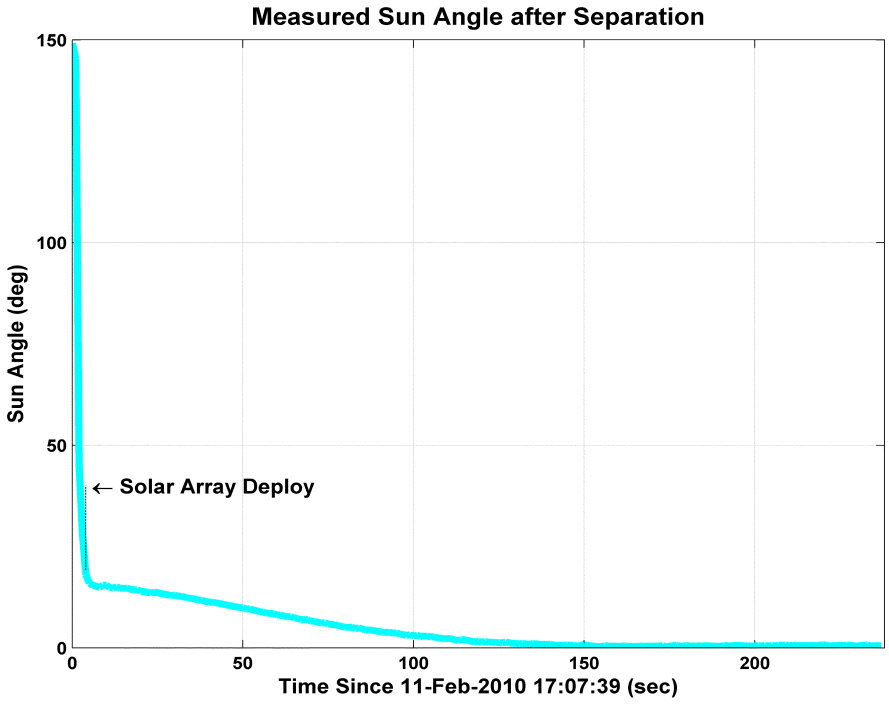

Figure 9: Post-Separation CSS Measured Sun Angles

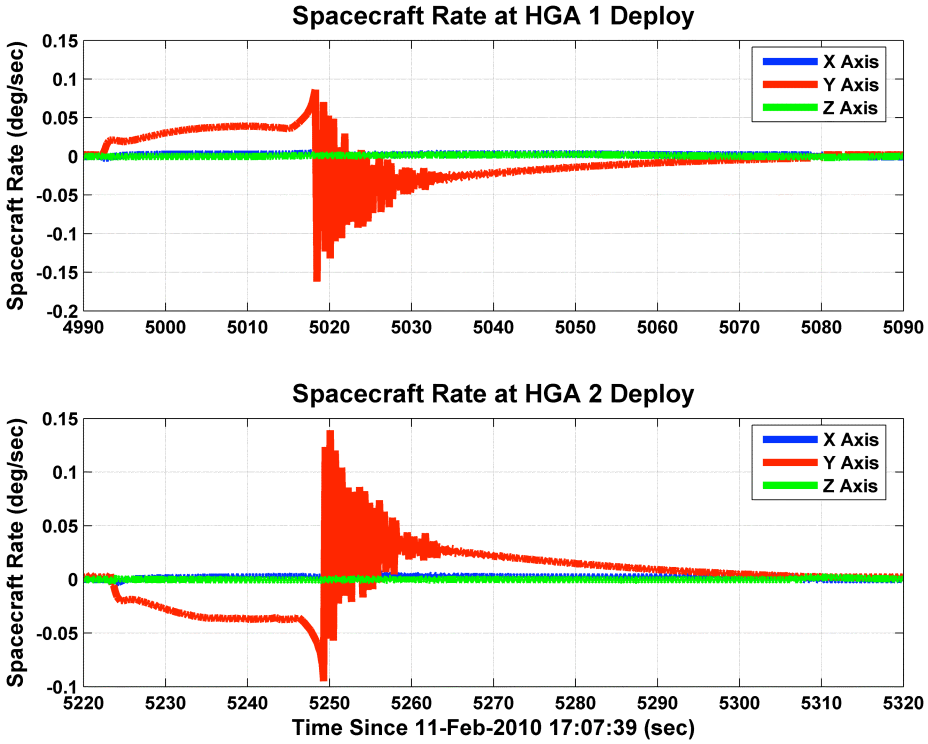

Figure 10: Spacecraft Rates at HGA Deployment

A. Initial ACS Checkout

One of the first post-separation and initial acquisition activities planned for SDO was a checkout of SDO's Safehold Mode. As the lowest level, minimum hardware component mode meant to ensure the safety of the spacecraft in the event of an anomaly, it was important to verify that the mode would work as designed. Additionally, because SDO has redundant ACE boxes in which Safehold is hosted, Safehold checkout was run on both ACEA and ACEB. The ACEA Safehold Mode test was run for ten minutes beginning at 21:50 GMT, followed immediately by a ten-minute test on ACEB. The plots shown in Figure 11 and Figure 12 are for the checkout of the ACEA Safehold Mode; ACEB yielded similar results.

SDO's Safehold Mode was designed to operate with a minimum sensor complement, meaning that the only sensor inputs that it normally uses are the output from the CSSs and from the RWA tachometers. Using just the CSS inputs, Safehold Mode is able to determine its position with respect to the Sun and is able to derive its rate about the two directions transverse to the sunline. When the spacecraft is close to Sun-pointing (within 15 degrees), Safehold Mode determines the X axis rate—the rate about the sunline—from the changing momentum in the reaction wheels. If the RWA momentum is too low, the derived rate is deemed unreliable and the X axis rate error in the Safehold controller is zeroed. This limit is 2 Nms for the root sum square of the Y and Z components of the RWA momentum in the body frame.

During Safehold checkout, the spacecraft saw sunline rates which cycled between high and low values. The spacecraft remained Sun-pointing, but the roll around the sunline alternated between periods of low roll rates and higher roll rates. This response is evident in the RWA momentum in the body frame plot shown in the upper section of Figure 11.

Downloaded by Scott Starin on September 21, 2012 | http://arc.aiaa.org | DOI: 10.2514/6.2011-6726

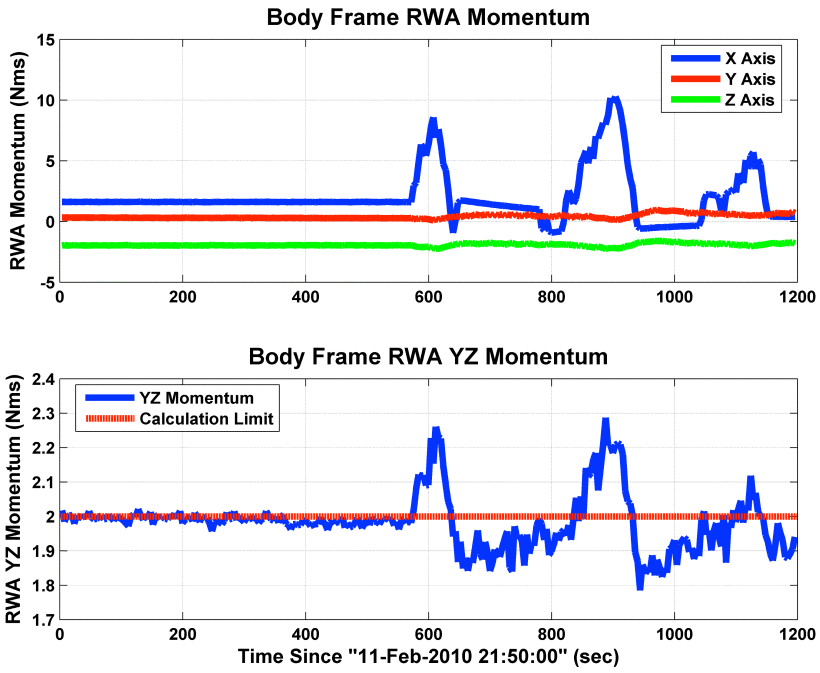

Figure 11: Safehold Checkout RWA Momentum in Body Frame

The lower plot of Figure 11 explains what is happening. When the YZ component of the RWA momentum is below 2 Nms, the sunline error rate fed to the Safehold controller is zeroed. By zeroing out the small rate, the true error in RWA momentum is allowed to build up without being counteracted by the controller. At some point, however, the accumulated momentum in the YZ plane exceeds 2 Nms and the controller begins reacting to it. As the controller reacts to the error and begins to lower it, the total YZ momentum will again go under 2 Nms. This reaction is what causes the alternating periods of lower and higher sunline rates during the Safehold test. Figure 12 shows the corresponding sunline rate signal used by the controller. At a higher overall system momentum, the sunline rate estimation algorithm would behave more consistently and the overall control would be better. At the low system momentum that the checkout test was run, which is more typical of SDO's operations, the Safehold Mode rate estimation and control algorithms are sufficient to safely and stably keep the spacecraft pointed at the Sun, which is power and thermally safe, as designed.

After checkout of Safehold Mode, the final "initial checkout" activity performed was polarity checks of the two sets of ACS thruster command paths. These polarity checks were performed while the spacecraft was in SunAcq Mode via manual thruster pulse commands sent to the ACE, with the results of each thruster firing being evaluated by the induced spacecraft rate and change in system momentum. The checkout was performed through both the ACEA and ACEB boxes, with enough 200-ms pulses fired on each thruster to get consistent results from one firing to the next, in an effort to blow out any bubbles that might have gotten into the propellant lines. The results of these tests showed nominal operation of all ACS thrusters through both ACE boxes.

Downloaded by Scott Starin on September 21, 2012 | http://arc.aiaa.org | DOI: 10.2514/6.2011-6726

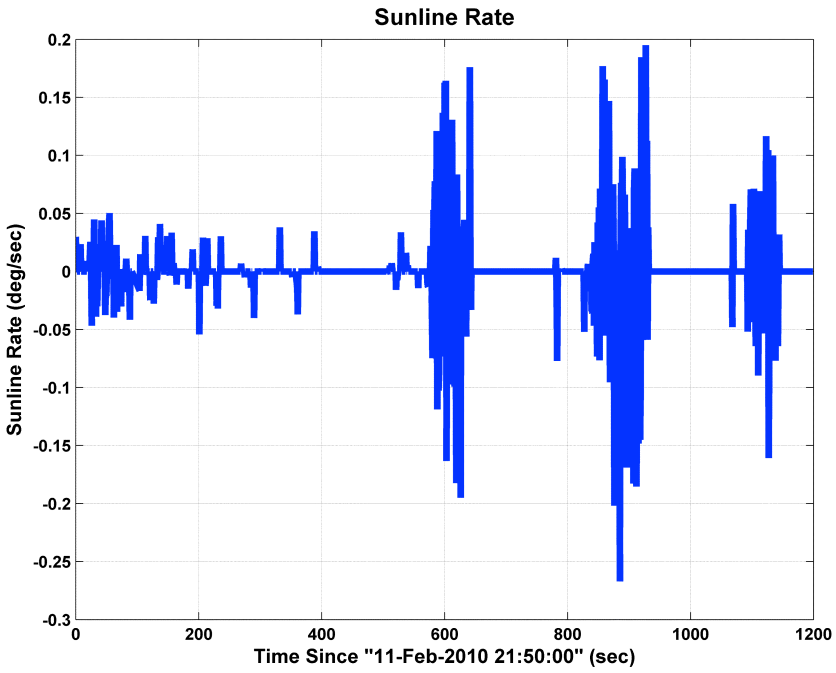

Figure 12: Safehold Checkout Calculated Sunline Error Rate

IV. Orbit Raising of the Solar Dynamics Observatory

The baseline plan to carry SDO from its initial GTO (8,800 km × 41,700 km) to its final geosynchronous orbit (42,164 km circular) of 102° west longitude and inclination of 28° consisted of ten maneuvers conducted over a period of three weeks: one engineering burn, six apogee motor firings (AMFs), where the primary ΔV would come from SDO's 110 lbf main engine, followed by three trim burns (TMFs) performed using ACS thrusters only. The engineering burn was designed as a short "dress rehearsal" for a full apogee motor firing. In the engineering burn and each of the AMFs, the first 20 seconds of the burn would use ACS thrusters only, with thrusters off-pulsing for attitude control; this would serve as a settling burn to push the propellant to the bottom of the tanks before the main engine kicked in. After this settling burn, the rest of the burn would include the main engine, with the ACS thrusters in an on-pulsing mode for attitude control. See Ref. 6 for a more complete description of the SDO orbit raising plan.

A. Propulsion System Commissioning and AMF-1

Due to heating concerns from one of the science instruments, the engineering burn was delayed from the nominal plan for four days, and was executed on February 15, at 02:42 GMT. Thruster polarity and rough thruster performance had been checked on launch day, so the only other propulsion system commissioning activity necessary before the engineering burn was to fire the pyrotechnic valves to pressurize the system. As shown in Figure 13, it was possible to see that the pyros had been fired based on disturbances to the spacecraft's attitude and rate.

Downloaded by Scott Starin on September 21, 2012 | http://arc.aiaa.org | DOI: 10.2514/6.2011-6726

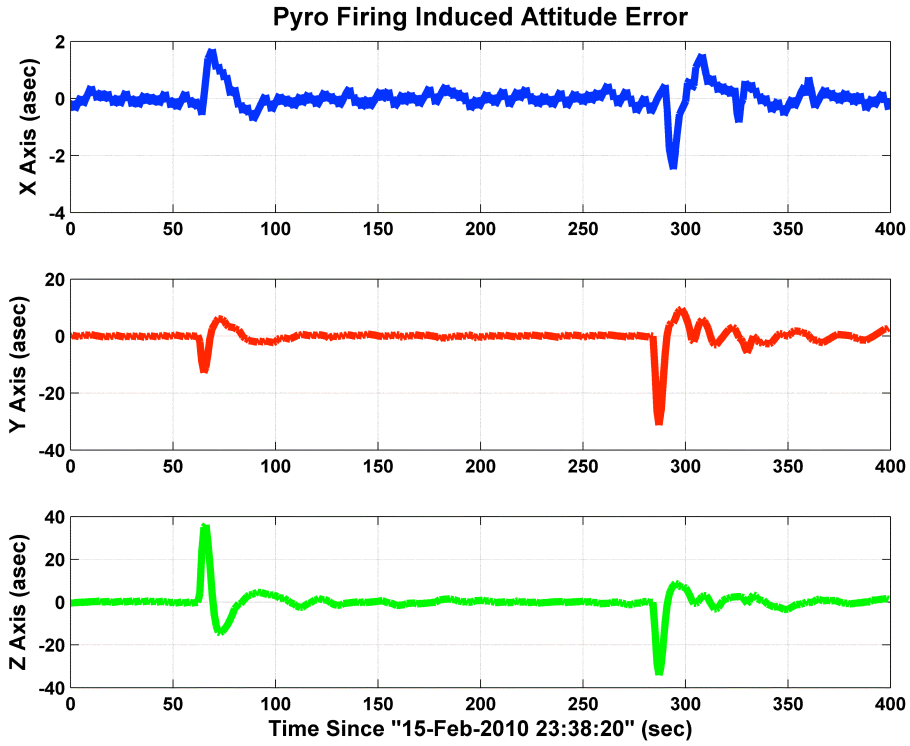

Figure 13: Attitude Error Induced by Firing Propulsion System Pyros

The ACS performance during the engineering burn was as expected, and the first AMF-1 was executed on February 17, with the burn starting at 22:15:28 GMT. The total length of the burn was 1133.4 seconds, slightly longer than the prelaunch plan, and completed successfully. The system momentum magnitude upon exit from DeltaV Mode was 3.07 Nms. Similar to the engineering burn, there were no failures or major problems during the maneuver. The only thing that occurred during the maneuver of potential serious concern was the fact that the KA-band electronic box temperature hit its red limit just before the burn finished. As a result, the flight dynamics team was directed to replan the remaining AMFs to limit the burn time to 20 minutes or less, and new operational constraints and procedures were defined for future AMFs in case the thermal limits were reached again.

B. Propellant Slosh Anomaly, Investigation, and Recovery

AMF-2 was planned to be a 1080 second burn beginning on February 19 at 21:55:32 GMT. The burn began on schedule, but approximately 37 seconds into the burn, the high system momentum FDC limit was tripped, aborting the burn and putting the spacecraft into SunAcq Mode. As designed, the safing scheme quickly slewed SDO to a safe, Sun-pointing attitude. The calculated system momentum, while high enough at around 23 Nms to trip the FDC limit during DeltaV Mode, was well within the capability of SunAcq. The first action of the flight support and maneuver teams after the anomaly was to ensure the safety of the spacecraft and clean up the state of the spacecraft telemetry status monitors (TSMs) and other FDC components that protect SDO while in SunAcq. Additionally, in order to reduce the relatively high momentum state of the spacecraft, manual thruster commands were performed to reduce the system momentum towards zero, with an as-expected momentum change occurring for each firing. After the spacecraft was safe, an anomaly team was formed to determine the cause of the DeltaV Mode anomaly.

The anomaly team identified a number of potential causes for the anomaly, including sensor failure, actuator (thruster or main engine) failure or previously unobserved misalignment, DeltaV Mode controller instability, other hardware failures, and unmodeled dynamics. Because of all the previous testing and examination of current data, there were not any sensor, actuator, or other hardware failures that seemed to be likely causes, and given its correct functioning during the engineering burn and AMF-1, DeltaV controller instability did not seem likely. After examining the system momentum and rate data during the aborted maneuver, it quickly became clear that the most likely cause of the anomaly was an unmodeled disturbance caused by propellant slosh.

Downloaded by Scott Starin on September 21, 2012 | http://arc.aiaa.org | DOI: 10.2514/6.2011-6726

Once the anomaly team successfully identified propellant slosh as the reason the burn was aborted, they began an intensive analysis and design effort to come up with a way to mitigate the slosh dynamics to allow the use of the main engine. Meanwhile, because SDO was in an unfavorable radiation environment and because the desire was to get the spacecraft into its science orbit as quickly as possible, the project decided to continue with its orbit raising effort, planning maneuvers using only the ACS thrusters. Because the ACS thrusters are much smaller and therefore less efficient, achieving the final science orbit without going back to the main engine would require an additional five or six burns and an additional two or more weeks. In parallel with the anomaly team work, three maneuvers—designated AMF-2B, AMF-3, and AMF-4—were performed using ACS thrusters only. All of these maneuvers were successful, though it should be noted that the attitude error during these maneuvers showed a more pronounced tendency towards a two-sided limit cycle in the Z axis. See Ref. 7 for specifics on the two-side limit cycle and all other details of the slosh anomaly investigation.

After completion of AMF-4 and extensive analysis effort, the anomaly team proposed three simple, easy-to-implement changes to the spacecraft that they felt would solve the problem. First, they suggested increasing the length of the settling burn from 20 seconds to four minutes. That length was selected to encompass the "geyser mode" that can be seen upon initial thruster firing, but did not allow enough time for fuel disturbances to damp out before the main engine firing. Second, the team suggested raising the FDC limit on system momentum to 34 Nms. The 20 Nms limit was chosen based on a two-failure scenario (how much momentum could be placed into the spacecraft by a stuck-on thruster and have the spacecraft successfully recover with one failed wheel); 34 Nms reflected a more realistic failure case. Finally, the team wanted to disable the effect of the structural filter, included in DeltaV Mode to allow it to meet the design requirement for 12 dB modal suppression of all flexible modes, by appropriately setting its parameters to ones and zeros. The increased phase delay caused by the structural filter was affecting DeltaV Mode's ability to react to the slosh dynamics, and the observed flexible modes and damping seen during the appendage deployments indicated that this could be done safely.

AMF-5 was the first post-anomaly maneuver to be performed with the main engine. In order to mitigate the operational effects of another failure, this maneuver was done as a "composite" maneuver: The 50 minute maneuver was planned as a 40-minute, ACS-thruster-only settling burn followed by the final 10 minutes using the main engine so that if using the main engine caused the maneuver to abort again, the overall maneuver would still impart a fair amount of ΔV to the spacecraft. To the relief of everyone on the project team, AMF-5 was a success. In fact, the changes made to mitigate the effect of the slosh dynamics—primarily the removal of the structural filter—significantly improved the response of the controller.

In summary, a total of 13 maneuvers (including the aborted AMF-2) were performed to move SDO into its mission orbit. After the engineering burn, the successful AMF-1 and the aborted AMF-2, three "AMFs" were performed using ACS thrusters only, followed by the main engine return-to-service composite AMF-5, three additional AMFs, and three TMF trims burns. The propellant slosh anomaly resulted in three additional maneuvers and a delay of only one week in achieving SDO's mission orbit. On March 16, at the conclusion of TMF-3, SDO achieved its final science orbit.

V. Attitude Control System Commissioning

While SDO's orbit raising activities were ongoing, and for another six weeks afterward, the commissioning, testing, and calibration of the ACS sensors, actuators, and control modes continued in parallel. The bulk of these tests consisted of ACS control mode checkouts and execution of slews used to calibrate the ACS sensors and actuators, as well as the science instruments and the AIA guide telescopes. In general, the results of these tests showed good performance of the ACS system, meeting all of its requirements. The remainder of this section discusses some of the interesting things discovered during the commissioning process, including some small performance puzzles that were solved.

A. Gyro Bias Oscillations

The day after launch, the major activities were the checkout of Inertial Mode, followed by a series of slews using that mode to provide data to calibrate the IRUs. Both of those activities were successful, but small spacecraft oscillations were observed in the IRU bias estimates calculated by the onboard Kalman filter, as shown in the plots in Figure 14. Because the oscillation was at such a low frequency, with a roughly 30 minute period, it was well within the bandwidth of the controller. Thus, the controller followed the oscillating error in the attitude estimate, resulting in actual spacecraft motion. Data from these tests, from subsequent tests of SDO Science Mode, and from all other suitable activities were examined. Even though the oscillations seen on all of the different tests were

Downloaded by Scott Starin on September 21, 2012 | http://arc.aiaa.org | DOI: 10.2514/6.2011-6726

approximately 10–20 arcsec and would not cause SDO's Science Mode to violate its pointing requirement of [35,70,70] arcsec, they remained a concern to the science instrument teams. It was determined by looking at this data that the IRUs were the cause, and that the frequency and the amplitude of the oscillations were temperature related. Eventually, the on-board attitude determination estimation was adjusted to filter the oscillations. Complete details on the analysis and mitigation of the gyro bias oscillations can be found in Ref. 8.

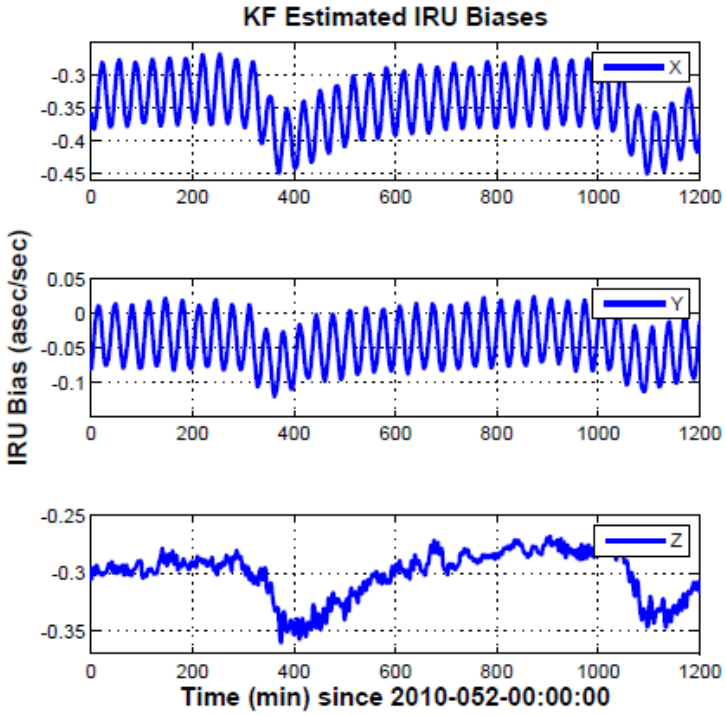

Figure 14: Attitude oscillations driven by IRU bias oscillations

B. Star Tracker Quality Index

The week prior to launch, the SDO team learned of an anomaly on the European Space Agency (ESA) mission, Herschel, where their GA star trackers, were accumulating "warm pixels" – pixels whose background energy level were higher than the energy levels of the surrounding pixels. The effect of these "warm pixels" was lower quality attitude solutions due to distortion on the image of the stars. As a tracked star nears a warm pixel, the ST Quality Index, a scalar value that represents the weighted average of the axis-by-axis solution covariance, will drop due to the higher energy level of the warm pixel blurring the image of the star. As the tracked star moves near the center of the warm pixel, the energy level of the star overwhelms that higher background level of the warm pixel and the Quality Index improves. Finally, as the tracked star moves away from the warm pixel, the star image again blurs and the Quality Index drops again. The resulting shape of the Quality Index over time, as the tracked star moves toward, across, and then away from a warm pixel, is that of an inverted "U" shape.

During commissioning, the ST Quality Index displayed this unusual shape. There was a period of approximately six hours during which the Quality Index showed an inverted "U" shape, dropping as low as 0.6 (on a scale of 0 to 1) at the beginning and end of the period and climbing back towards 0.95 (the nominal, expected value) during the middle of the period. The investigation into the anomalous ST Quality Index behavior is described in Ref.s 8 and 9.

C. Coarse Sun Sensor Sun Angle Calculation

During the engineering burn and AMF-1, the FDC limit for a Sun vector mismatch (a three-way comparison between CSSA, CSSB, and AD calculated vectors) tripped multiple times. Though the persistence of these limit violations were not nearly long enough to trip any autonomous FDC actions, the team was interested in understanding why they were occurring.

Downloaded by Scott Starin on September 21, 2012 | http://arc.aiaa.org | DOI: 10.2514/6.2011-6726

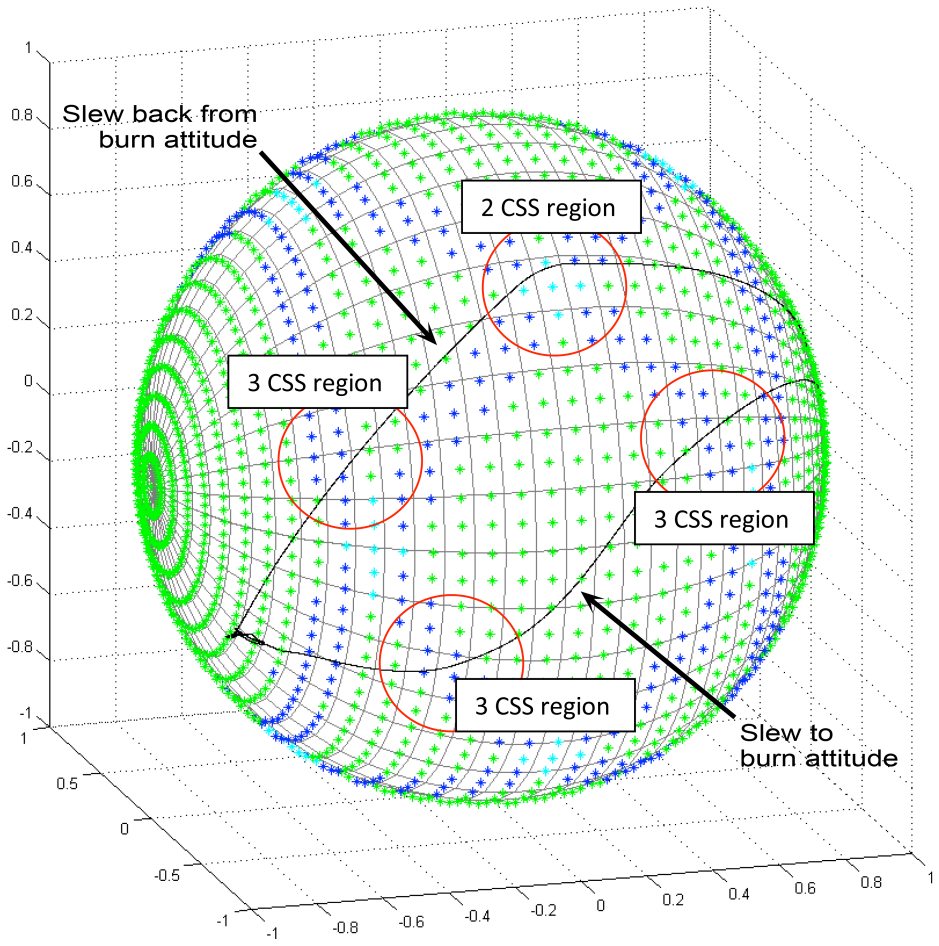

Figure 15: CSS Coverage Map During AMF-1 Slews

Figure 15 shows the unit sphere of possible Sun vectors in the SDO body reference frame. The dark lines superimposed on the sphere represent the attitude path taken by SDO as it slewed out to the burn attitude for AMF-1 and then back to pointing at the Sun afterwards. The colors of the points on the sphere represent how many individual CSSs register sunlight at each point. The green areas are regions of 4-sensor coverage, the blue areas are regions of 3-sensor coverage, and the cyan areas are regions of 2-sensor coverage. Different algorithms are used to calculate the Sun vector for the 4-sensor case than the 3- and 2-sensor cases. During nominal science data collection, four CSSs have visibility of the Sun, and it is in this condition where the calculation of the Sun angle is the most accurate. As shown on the figure, there are several locations along the path where only two or three CSSs can see the Sun. It is in these zones that the limit trips occurred. On both ACEs, the times of CSSA vs CSSB mismatches occurred during times of decreased Sun coverage. In the regions where fewer than four sensors are used, the comparison between CSSA and CSSB is more likely to be different, primarily because the two ACEs may transition between the 4-sensor and 3-sensor algorithms at a slightly different times.

VI. On-Orbit Jitter Testing

Two of the SDO instruments, Atmospheric Imaging Assembly (AIA) and Helioseismic and Magnetic Imager (HMI), are sensitive to high frequency pointing perturbations and have sub-arcsecond level line-of-sight (LOS) jitter requirements. Extensive modeling and analysis efforts were directed in estimating the amount of jitter disturbing the science instruments and designing jitter reducing operational features.[10,11,12,13] A jitter test plan was developed to verify analysis approaches and reduce uncertainties in the models. This plan consisted of hardware component tests, structural component tests, and assembly level tests. The hardware component test results were used for calibrating the disturbance input models that drove the observatory structural and optical models used to predict the LOS jitter performance.

Although detailed analysis and assembly level tests were performed to obtain good jitter predictions, there were still several sources of uncertainty in the system. The structural finite element model did not have all the modes correlated to test data at high frequencies (>50 Hz). The performance of the instrument stabilization system was not known exactly, but was expected to be close to the analytical model. A true disturbance-to-LOS observatory level

Downloaded by Scott Starin on September 21, 2012 | http://arc.aiaa.org | DOI: 10.2514/6.2011-6726

test was not available due to the tight schedule of the flight spacecraft, the cost in time and manpower, difficulties in creating gravity negation systems, and risks of damaging flight hardware. To protect the observatory jitter performance against model uncertainties, the SDO jitter team devised several on-orbit jitter reduction plans in addition to reserving margins on analysis results. Since some of these plans severely restricted the capabilities of several spacecraft components (e.g. wheels and high gain antennas), the SDO team performed on-orbit jitter tests to determine which jitter reduction plans, if any, were necessary to satisfy science LOS jitter requirements.

Towards the end of early operations, after the ACS calibration and instrument commissioning was complete, a three-day test period was dedicated to measure AIA and HMI LOS jitter induced by various spacecraft and instrument mechanisms. Ref.s 14 and 15 describe the jitter test methodology, compare the on-orbit measured and pre-launch predicted LOS jitter, and document the final operational configuration for all jitter mitigation features.

VII. On-Orbit Momentum Management

Jitter being a special concern well before launch, every aspect of spacecraft design and operation was examined carefully to find ways of satisfying jitter requirements. In the analysis of the contribution of reaction wheels to the total jitter picture, it was found that keeping the wheels below a speed of approximately 400 RPM (~5 Nms) would reduce tonal disturbances that were of major concern. As can be read in detail in Ref. 10 and 11, limiting wheel speed by no means solved all the jitter problems, but it provided a big enough improvement that a detailed analysis of the feasibility of maintaining these low speeds for all science operations was undertaken. This proposed operational plan represented a large change from the expected operational speeds of approximately 2400 RPM (~30 Nms). The idea was to use projected ephemeris and attitude information to predict angular momentum build-up over the four weeks following a planned momentum management maneuver. Then, a target momentum in the opposite direction of the prediction was determined such that, if the prediction were correct, the wheel speeds would decrease for approximately two weeks, change direction, and then gradually increase over the following two weeks until the next momentum management maneuver could repeat the cycle. In this way, maximum wheel speeds would be minimized. Details of the pre-launch analysis and the momentum management plan that resulted can be found in Ref. 5.

After launch, some adjustments were made to the momentum management plan. Early in the orbit raising part of operations, disturbance torques on the observatory were much larger than would be seen in the GEO orbit, but this was expected and acceptable, because engineering (i.e. non-science) operations are not appreciably affected by jitter. This period of jitter-insensitive time was used by the GNC and flight operations specialists to test their procedures and scripts for precisely placing angular momentum in the observatory. The main method expected before launch was to use the closed-loop DeltaH control mode for these maneuvers, but an open-loop method was developed shortly before launch and improved after launch. This method was to use a spreadsheet with thruster position and thrust vector information to determine an open-loop set of direct processor commands to place momentum using individual ACS thrusters. DeltaH performed as expected and required, but the open-loop method was found to be more precise in the final momentum established, so the open-loop method was used throughout most of the commissioning period. After commissioning was over and a comfortable pace of operations had been established, momentum management maneuvers used the slightly less precise but much less labor intensive, closed-loop, DeltaH method.

By the end of commissioning, DeltaH demonstrated the ability to precisely place a commanded momentum vector in the spacecraft body frame. Further, as a result of on-orbit jitter testing, the maximum allowable speed for each wheel was increased to 850 RPM (~10 Nms)[15]. This increased allowable range has resulted in fewer DeltaH maneuvers being required, minimizing the interruptions to science observations. However, DeltaH's performance is a separate concern from predicting the evolution of the momentum state. Knowledge of the momentum trend is necessary to backsolve for the most benefical commanded momentum vector and required development of a special set of tools[6] for which improvements are ongoing.

VIII. Conclusion

On May 17, 2010, the SDO Project Manager Liz Citrin "handed over the keys" of SDO to Space Science Mission Operations, signifying the successful conclusion of commissioning and the formal beginning of its science mission. As early as March 31, though, when AIA captured the First Light image shown in Figure 23, SDO was destined for

Downloaded by Scott Starin on September 21, 2012 | http://arc.aiaa.org | DOI: 10.2514/6.2011-6726

success. Due to the robust design of the ACS subsystem and with the skill and dedication of the flight support team in diagnosing the anomalies seen in flight, the SDO ACS was a key factor in this success.

Acknowledgements

The authors wish to acknowledge Thomas M. Kenney for his GNC Systems engineering work during design and test, and David K. Ward and P. Michael Bay for their Systems engineering support during design, test, and on-orbit commissioning.

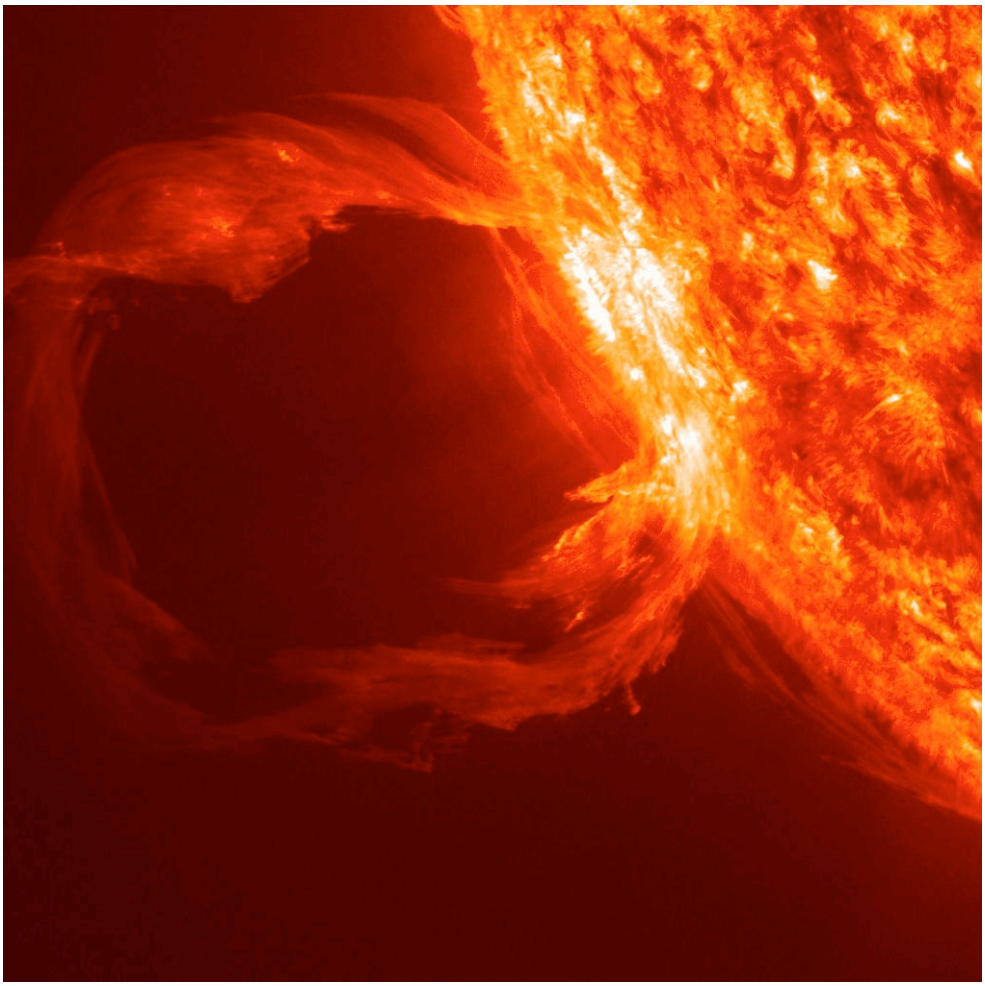

Figure 16: First Light Image from the SDO AIA Instrument taken on March 30, 2010

References

[1] Scott R. Starin, Kristin L. Bourkland, Kuo-Chia Liu, Paul A. C. Mason, Melissa F. Vess, Stephen F. Andrews, and Wendy M. Morgenstern. "Attitude Control System Design for the Solar Dynamics Observatory." Flight Mechanics Symposium, 2005.

[2] Scott R. Starin, Melissa F. Vess, Thomas M. Kenney, Manuel D. Maldonado, and Wendy M. Morgenstern. "Fault Detection and Correction for the Solar Dynamics Observatory Attitude Control System." AAS Guidance and Control Conference, Breckenridge, CO, 2008.

[3] Kristin L. Bourkland, Scott R. Starin, and David J. Mangus. "The Use of a Gyroless Wheel-Tach Controller in SDO Safehold Mode." Flight Mechanics Symposium, 2005.

Downloaded by Scott Starin on September 21, 2012 | http://arc.aiaa.org | DOI: 10.2514/6.2011-6726

[4] Melissa F. Vess, Scott R. Starin, and Wendy M. Morgenstern. "Use of the SDO Pointing Controllers for Instrument Calibration Maneuvers." Flight Mechanics Symposium, 2005.

[5] Paul A. C. Mason and Scott R. Starin. "SDO Delta H Mode Design and Analysis." International Symposium on Space Flight Dynamics, 2007.

[6] Neil Ottenstein, Greg Natanson, Richard McIntosh, Joe Hashmall, Seth Shulman, Robert DeFazio, Scott Starin, Kristin Bourkland, Paul Mason, and Melissa Vess. "Solar Dynamics Observatory (SDO) Ascent Planning and Momentum Management." Space Ops 2010, Huntsville, AL, 2010.

[7] P. Mason, S. R. Starin. The Effects of Propellant Slosh Dynamics on the Solar Dynamics Observatory. AIAA Guidance, Navigation, and Control Conference, 8-11 August 2011, Portland, Oregon.

[8] Melissa. F. Vess, Scott R. Starin, Kuo-Chia Liu. "Investigating On-Orbit Attitude Determination Anomalies for the Solar Dynamics Observatory Mission." AIAA Guidance, Navigation, and Control Conference, 8-11 August 2011, Portland, Oregon.

[9] Denis Felikson, Matt Ekinci, Joseph. A. Hashmall, Melissa F. Vess. "On-Orbit Solar Dynamics Observatory (SDO) Star Tracker Warm Pixel Analysis." AIAA Guidance, Navigation, and Control Conference, 8-11 August 2011, Portland, Oregon.

[10] Kuo-Chia (Alice) Liu, Thomas Kenney, Peiman Maghami, Pete Mule, Carl Blaurock, and William B. Haile. "Jitter Test Program and On-Orbit Mitigation Strategies for Solar Dynamics Observatory." International Symposium on Space Flight Dynamics, 2007.

[11] Kuo-Chia Liu, Peiman Maghami, and Carl Blaurock. "Reaction Wheel Disturbance Modeling, Jitter Analysis, and Validation Tests for Solar Dynamics Observatory." AIAA Guidance, Navigation and Control Conference and Exhibit, August 2008, Honolulu, Hawaii. AIAA 2008-7232.

[12] Kristin L. Bourkland, Kuo-Chia (Alice) Liu, and Carl Blaurock. "A Jitter-Mitigating High Gain Antenna Pointing Algorithm for the Solar Dynamics Observatory." International Symposium on Space Flight Dynamics, 2007.

[13] Carl Blaurock, Kuo-Chia Liu, and Peter Mule. "Solar Dynamics Observatory (SDO) HGAS Induced Jitter." 49th AIAA/ASME/ASCE/AHS/ASC Structures, Structural Dynamics, and Materials Conference, 2008, AIAA 2008-1951.

[14] Kristin L. Bourkland, Kuo-Chia (Alice) Liu. "Verification of the Solar Dynamics Observatory High Gain Antenna Pointing Algorithm Using Flight Data." AIAA Guidance, Navigation, and Control Conference, 8-11 August 2011, Portland, Oregon.

[15] Kuo-Chai (Alice) Liu, Carl. A. Blaurock, Kristin Bourkland, Wendy Morgenstern, Peiman. G. Maghami. "Solar Dynamics Observatory On-orbit Jitter Testing, Analysis, and Mitigation Plans." AIAA Guidance, Navigation, and Control Conference, 8-11 August 2011, Portland, Oregon.

Downloaded by Scott Starin on September 21, 2012 | http://arc.aiaa.org | DOI: 10.2514/6.2011-6726